AWARD NUMBER: W81XWH-17-1-0652

TITLE: Temporal Evolution of N-Myc Signaling and Early Targeting of the Neuroendocrine Phenotype in Prostate Cancer

PRINCIPAL INVESTIGATOR: Drs. David Rickman, Himisha Beltran

RECIPIENT: David Rickman

REPORT DATE: OCTOBER 2021

TYPE OF REPORT: Annual Technical Report

PREPARED FOR: U.S. Army Medical Research and Materiel Command
Fort Detrick, Maryland 21702-5012

DISTRIBUTION STATEMENT: Approved for Public Release; Distribution Unlimited

The views, opinions and/or findings contained in this report are those of the author(s) and should not be construed as an official Department of the Army position, policy or decision unless so designated by other documentation.

REPORT DOCUMENTATION PAGE

Form Approved
OMB No. 0704-0188

Public reporting burden for this collection of information is estimated to average 1 hour per response, including the time for reviewing instructions, searching existing data sources, gathering and maintaining the data needed, and completing and reviewing this collection of information. Send comments regarding this burden estimate or any other aspect of this collection of information, including suggestions for reducing this burden to Department of Defense, Washington Headquarters Services, Directorate for Information Operations and Reports (0704-0188), 1215 Jefferson Davis Highway, Suite 1204, Arlington, VA 22202-4302. Respondents should be aware that notwithstanding any other provision of law, no person shall be subject to any penalty for failing to comply with a collection of information if it does not display a currently valid OMB control number. **PLEASE DO NOT RETURN YOUR FORM TO THE ABOVE ADDRESS.**

1. REPORT DATE	2. REPORT TYPE	3. DATES COVERED
Oct 2021	Annual	30 Sep 2020 - 29 Sep 2021

4. TITLE AND SUBTITLE

Temporal Evolution of N-Myc Signaling and Early Targeting of the Neuroendocrine Phenotype in Prostate Cancer

5a. CONTRACT NUMBER

5b. GRANT NUMBER
W81XWH-17-1-0652

5c. PROGRAM ELEMENT NUMBER

6. AUTHOR(S)
Dr. David Rickman; Himisha Beltran

Email: dsr2005@med.cornell.edu

5d. PROJECT NUMBER

5e. TASK NUMBER

5f. WORK UNIT NUMBER

7. PERFORMING ORGANIZATION NAME(S) AND ADDRESS(ES)

Weill Medical College of Cornell University

New York, NY 10065

8. PERFORMING ORGANIZATION REPORT NUMBER

9. SPONSORING / MONITORING AGENCY NAME(S) AND ADDRESS(ES)
U.S. Army Medical Research and Materiel Command
Fort Detrick, Maryland 21702-5012

10. SPONSOR/MONITOR'S ACRONYM(S)

11. SPONSOR/MONITOR'S REPORT NUMBER(S)

12. DISTRIBUTION / AVAILABILITY STATEMENT
Approved for Public Release; Distribution Unlimited

13. SUPPLEMENTARY NOTES

14. ABSTRACT:

While therapies targeting the androgen receptor (AR) have significantly improved outcomes for men with advanced prostate cancer, it has been increasingly recognized that a subset of castration resistant tumors lose dependence or 'escape' AR signaling which is associated with epithelial plasticity, loss of AR mRNA and protein expression, and the development of neuroendocrine features. Castration resistant neuroendocrine prostate cancer (NEPC) is clinically aggressive and median survival is less than one year. The poor prognosis of NEPC can be accounted for, in part, by late diagnosis and an incomplete understanding of the molecular events underlying its pathogenesis. Over the last 7 years, our groups have co-led extensive molecular analyses of NEPC, elucidated mechanisms of clonal evolution, and have identified the oncogenic transcriptional factor N-Myc as a key driver of the neuroendocrine phenotype (Beltran, Rickman et a, Cancer Discovery 2011; Dardenne, Beltran et al, Cancer Cell, in press). Notably we found that NEPC is clonally derived with an origin traceable back to a prostate adenocarcinoma precursor, providing new potential opportunities for early detection and potentially early intervention. Through the development of multiple N-Myc-overexpressing prostate cancer preclinical models, we have found that N-Myc drives NEPC by inducing a profile enriched with pro-metastatic, dedifferentiation and Polycomb Repressive Complex 2 (PRC2) dysregulated genes and dramatically reducing AR signaling

15. SUBJECT TERMS

NONE LISTED

16. SECURITY CLASSIFICATION OF:			17. LIMITATION OF ABSTRACT	18. NUMBER OF PAGES	19a. NAME OF RESPONSIBLE PERSON
a. REPORT	b. ABSTRACT	c. THIS PAGE			USAMRMC
U	U	U	UU	32	19b. TELEPHONE NUMBER *(include area code)*

TABLE OF CONTENTS

	Page No.
1. Introduction	1
2. Keywords	1
3. Accomplishments	2
4. Impact	19
5. Changes/Problems	23
6. Products	24
7. Participants & Other Collaborating Organizations	26
8. Special Reporting Requirements	29
9. Appendices	29

1. **INTRODUCTION:** Narrative that briefly (one paragraph) describes the subject, purpose and scope of the research.

Lineage plasticity and histologic transformation of prostate cancer to a small cell neuroendocrine prostate cancer (NEPC) has emerged as a resistance mechanism in a subset of patients with metastatic prostate cancer following exposure to androgen receptor (AR)-targeted therapies. NEPC is associated with low or absent AR expression, suppressed AR signaling, retention of early genomic mutations from its adenocarcinoma precursor, and acquisition of distinct genomic and epigenomic alterations (Beltran H, et al, Nature Medicine, 2016). The development of novel therapeutic approaches for patients with NEPC represents a clinical unmet need. Over the last ten years, we have worked together to characterize the molecular landscape of NEPC and have identified and validated new therapeutic targets, including the N-Myc/Aurora A pathway and specific epigenetic modifiers such as (Enhancer of Zeste Homolog 2) EZH2 (Beltran H, Rickman DS et al Cancer Discovery 2011; Dardenne E, Beltran H, …. and Rickman DS, Cancer Cell 2016).

Hypothesis: N-Myc is an early driver of the NEPC phenotype, and that by tracking N-Myc signaling during the transition from adenocarcinoma to NEPC, we can identify cooperating factors that promote NEPC progression and define appropriate time points for early intervention.

To address this hypothesis, we formulated 3 Specific Aims:

Specific Aim 1: To assess the timing of N-Myc activation in patients and define how N-Myc and NEPC signaling impacts prognosis. The working hypothesis of this **Aim** is that there are specific molecular changes that serve as early markers of tumors that will evolve to NEPC. We will assess patient tumors at various timepoints during disease progression from prostate adenocarcinoma to NEPC and correlate N-Myc expression and NEPC signaling with clinical features and outcomes. We will also investigate MYCN and AURKA genomic amplification in tumors and circulating tumor DNA (ctDNA). Specifically, we will evaluate: 1) localized prostate cancer patients treated with prostatectomy; 2) high risk localized patients treated with or without neoadjuvant docetaxel and androgen deprivation therapy (NCT00430183); 3) patients with metastatic CRPC treated with abiraterone, and enzalutamide (IRB1305013903, PI Beltran); 4) NEPC patients treated with the Aurora A inhibitor MLN8237 (NCT01799278, PI Beltran). Gene expression will be quantified using a custom-designed assay validated by our group and amenable to FFPE tissues. N-Myc, Aurora A, and AR signaling genes, stem cell, neuronal, and other NEPC markers will be assessed. AURKA and MYCN amplification will be evaluated in tumors and ctDNA by targeted exome sequencing and/or FISH. We predict that N-Myc/NEPC signaling may be detected early in a subset of high-risk patients and this represents the presence of treatment resistant cells, and that this signaling program is enhanced after both short and long term AR-targeted therapies. The detection and determination of the frequency of early NEPC-associated alterations will help molecularly define subsets of prostate adenocarcinomas as harbingers of NEPC. This has clinical implications towards the development of diagnostic, prognostic, and predictive biomarkers to be evaluated early (potentially at the time of prostate cancer diagnosis) to select individuals at high risk for progression for early intervention. These results will also help identify patients less likely to benefit from AR-targeted strategies and more likely to benefit from MLN8237 or other N-Myc directed approaches.

Specific Aim 2: To assess the impact of timing of N-Myc expression on the development of castration resistance and the NEPC phenotype. The working hypothesis of this **Aim** is that N-Myc drives the trans-differentiation of castration resistant adenocarcinomas towards the NEPC phenotype. In order to model the evolutionary acquisition of N-Myc signaling during prostate cancer progression, we will temporally regulate N-Myc expression either at (3 months) or after (6 months and 9 months) the time of disease onset following Pten deletion both in intact mice and in mice castrated at 6 months. We will monitor Pten mutant cells (using YFP) before N-Myc and after N-Myc (Td-Tomato) overexpression and lineage trace emerging clones that develop

histological and molecular features of NEPC. We expect that castration will lead to a quicker N-Myc-induced onset of NEPC.

Specific Aim 3: To evaluate the influence of N-Myc timing on response to NEPC directed therapeutics. The working hypothesis of this **Aim** is that N-Myc over-expression sensitizes CRPC to NEPC-directed therapeutics. We will test N-Myc-early and N-Myc-late models with drugs that have demonstrated efficacy against NEPC including Aurora kinase A inhibition, platinum chemotherapy and EZH2 inhibitors. We will also evaluate the effect of the EZH2 inhibitors as priming agents with Aurora-A or AR-directed therapies (enzalutamide) in delaying or reversing AR-independent resistance *in vitro* and *in vivo*. We predict that early N-Myc expression results in comparable response to N-Myc targeted therapies as NEPC and early treatment with these agents modulates NEPC transcriptional programs. Results from this **Aim** will aid in biomarker selection for future trials.

2. KEYWORDS: Provide a brief list of keywords (limit to 20 words).

Castration resistant prostate cancer (CRPC), androgen receptor (AR)-targeted therapy, neuroendocrine prostate cancer (NEPC), N-Myc transcription factor (N-Myc), Polycomb Repressive Complex 2-associated protein Enhancer of Zeste Homolog 2 (EZH2).

3. ACCOMPLISHMENTS: The PI is reminded that the recipient organization is required to obtain prior written approval from the awarding agency Grants Officer whenever there are significant changes in the project or its direction.

What were the major goals of the project?

a. Major goals of the project

1. Specific Aim 1: To assess the timing of N-Myc activation in patients and define how N-Myc signaling impacts response to aurora kinase A inhibition and clinical outcomes.
    a. Evaluate localized prostate cancer patients treated with prostatectomy
    b. Evaluate high risk localized patients treated with or without neoadjuvant docetaxel and androgen deprivation therapy (NCT00430183).
    c. Evaluate pre-treatment metastatic biopsies from CRPC patients treated with abiraterone, and enzalutamide (IRB1305013903).
    d. Evaluate pre-treatment metastatic biopsies from NEPC patients treated with the Aurora A inhibitor MLN8237 (NCT01799278) on a Phase 2 clinical trial or the EZH2 inhibitor GSK126 (NCT02082977).

2. Specific Aim 2: Assess the impact of timing of N-Myc expression on the development of castration resistance and the NEPC phenotype.
    a. Assess the influence of N-Myc on the onset of CRPC and NEPC and associated molecular changes.
    b. Assess the role of N-Myc/EZH2 complex for N-Myc dependent transcriptional regulation in establishing the NEPC phenotype.
    c. Assess the role of N-Myc/Aurora-A complex for N-Myc dependent

transcriptional regulation in establishing the NEPC phenotype

3. Specific Aim 3: Determine the impact of the timing of N-Myc on response to NEPC directed therapeutics.
    a. Monitor the impact of the timing of N-Myc expression in response to NEPC-related monotherapies *in vivo* and *in vitro.*
    b. Monitor the impact of the timing of N-Myc expression in response to NEPC-related combination therapies *in vivo* and *in vitro.*
    c. Mechanistic studies to determine NEPC-related molecular changes associated with EZH2 and Aurora A inhibition *in vitro* and *in vivo*

b. Accomplishments under these goals

1. Specific Aim 1: To assess the timing of N-Myc activation in patients and define how N-Myc signaling impacts response to aurora kinase A inhibition and clinical outcomes.

High *MYCN* expression and *RB1* deletion are prognostic in patients with metastatic CRPC and NEPC

76 patient biopsies were grouped according to their tumor histological classification (CRPC or NEPC) and stratified into three categories based on RNA-seq values of *MYCN* expression (high vs. low) and *RB1* genomic status (deletion, yes vs. no). Of the 76 patient samples, 55 were histologically classified as CRPC and 21 as NEPC. We observed that 19/76 (25%) of patients had tumors with high N-Myc expression and *RB1* deletion. Overall 9/55 (16.4%) CRPC and 10/21 (47.6%) NEPC had high N-Myc expression and *RB1* deletion, suggesting that co-occurrence of N-Myc overexpression and *RB1* loss may be enriched for during development of NEPC (**Figure 1A**). Moreover, we observed that high N-Myc expression in combination with *RB1* deletion in patient CRPC and NEPC tumors was significantly associated with a worse overall survival compared to those with high N-Myc expression/*RB1* normal or low N-Myc expression/*RB1* normal (19.93 months (range between 1.83-81.5 months) versus 32.27 (6.6-87.17) or 42.90 (4.2-145.3) months, p=0.03). Our data showed that the co-occurrence of both high N-Myc expression and *RB1* deletion predicted an overall worse prognosis. Several studies have investigated the role of N-Myc overexpression [1-4] or RB loss [5,6] in driving the development of NEPC, however, the possible synergistic role, if any, of these genetic alterations as drivers has not been reported.

We profiled circulating tumor cells (CTCs) by single-cell whole genome sequencing and immunofluorescence, collected from patients with CRPC and NEPC using the Epic assay (Conteduca et al, NPJ Oncology 2021). We found that while tumor suppressor loss can be seen in advanced prostate cancer patients regardless of histology, co-occurrence of PTEN/RB1/TP53 loss in single CTCs (versus different CTCs) was more common in NEPC. In addition, concurrent tumor suppressor loss was associated with higher NE marker expression and lower AR expression (**Figure 1**)

We are in the process of RNA/DNA profiling a cohort of high risk localized prostate cancers from patients enrolled on a Phase 3 trial (NCT00430183) to assess the frequency and clinical impact of N-myc expression with or without tumor suppressor alterations in untreated high risk prostate cancer.

2. Specific Aim 2: Assess the impact of timing of N-Myc expression on the development of castration resistance and the NEPC phenotype.

MYCN+ and *Rb1* deletion accelerates progression to AR-negative, poorly differentiated/NEPC tumors, metastases, and decreased median survival.

To determine the impact of N-Myc overexpression and *Rb1* loss on tumor progression *in vivo*, we introduced $Rb1^{f/f}$ alleles into our previously described $Pb\text{-}Cre4^{+/-};Pten^{f/f};LSL\text{-}MYCN^{+/+}$ genetically engineered mouse (GEM) model [3]. For simplicity, we will refer to the different genotypes and controls with aliases (**Figure 2B**). Similar to the clinical cases, both $MYCN+;Rb1^{f/+}$ and $MYCN+;Rb1^{f/f}$ mice had a poorer survival (median survival time of 12.5 weeks ($MYCN+;Rb1^{f/f}$ mice) or 19 weeks ($MYCN+;Rb1^{f/+}$ mice)) compared to *MYCN*+ mice (median survival time of 26 weeks) and $Rb1^{f/f}$ mice (38 weeks, **Figure 2C** [5]). Additionally, $MYCN+;Rb1^{f/f}$ and $MYCN+;Rb1^{f/+}$ mice developed large, invasive tumors with AR-negative and poorly differentiated foci as early as 8 weeks ($MYCN+;Rb1^{f/f}$) or 12 weeks ($MYCN+;Rb1^{f/+}$), respectively. These foci were positive for the neuroendocrine marker INSM1 [7,8], EZH2, as well as NKX2-1, a marker associated with small cell neuroendocrine carcinomas (including prostate) [7-9]. **(Figure 2D, E**). Based on hematoxylin and eosin staining, some of these foci displayed condensed nuclei and scant cytoplasm, characteristics of NEPC morphology. These tumors also included other foci of divergent differentiation (i.e. intestinal and squamous) as well as conventional, AR positive, adenocarcinoma similar to *MYCN*+ primary tumors previously described [2,3] but the percentage of conventional adenocarcinoma decreased over time while the percentage of poorly differentiated histology increased over time. This is in contrast to *MYCN*+ or $Rb1^{f/f}$ tumors, which had primarily high-grade prostatic intraepithelial neoplasia (HGPIN) at the earlier time points.

We also found that the different genotypes were associated with different metastatic potentials (summarized in **Figure 2E**). Lung and liver metastatic lesions were AR negative, however, lymph node metastatic lesions contained both AR positive and negative tumor cells, suggesting that loss of AR expression is not necessary for metastasis. Additionally, both lung and lymph node lesions were RB1-positive, further suggesting that complete loss of *Rb1* is not necessary to provide metastatic potential. We also found that the onset of metastasis for $MYCN+;Rb1^{f/f}$ mice, occurring as early as 8 weeks, was significantly accelerated compared to *MYCN*+ [2,3] or $Rb1^{f/f}$ [5] mice. By 12 weeks, 100% of $MYCN+;Rb1^{f/f}$ intact mice developed distant metastatic lesions (n=8). Metastases to the lung, liver, lymph nodes, and kidney primarily consisted of large and small cell neuroendocrine histologies that stained positive for INSM1 and N-Myc but negative for AR. These data suggest that *Rb1* loss in the context of *MYCN*+ accelerates the formation of poorly differentiated tumors with high metastatic potential, and eventually NEPC.

To determine if *Rb1* loss promotes castration resistance in the context of *MYCN*+, we performed longitudinal magnetic resonance imaging (MRI) analyses to track tumor growth before and after castration at 12 weeks of age. Based on both coronal and axial MRI-based tumor volume measurements, $MYCN+;Rb1^{f/f}$ mice did not respond to surgical castration and continued to grow rapidly (**Figure 2F**). In contrast, tumors in $Rb1^{f/f}$, *MYCN*+, and CTRL mice regressed post-castration. As expected, we found that *MYCN*+ and $Rb1^{f/f}$ tumors resumed growth 24 weeks post-castration whereas CTRL tumors did not show tumor regrowth at 52 weeks of age, consistent with previous reports [3,5]. In castrated mice, the median survival time was reduced for $MYCN+;Rb1^{f/f}$ (24 weeks) compared to $Rb1^{f/f}$ (43.5 weeks) and *MYCN*+ (44 weeks) mice). In addition, post-castration tumors from $MYCN+;Rb1^{f/f}$ mice harbored foci enriched with divergent differentiated histology compared to adenocarcinoma and increased metastatic potential compared to $Rb1^{f/f}$ and *MYCN*+ mice.

To determine if the local prostate microenvironment is essential for the observed phenotypes, we derived three-dimensional from normal prostate epithelial tissue obtained from 7

to 8-week old *Pb-Cre4*-negative GEMs and transduced them *in vitro* with a Cre-expressing adenovirus. Immunoblot and IHC analyses confirmed the presence of functional alleles following Cre induction and confirmed that all GEM-derived organoids were positive for AR. We injected *MYCN+*^{Cre} and *MYCN+;Rb1*$^{f/f Cre}$ organoids subcutaneously into nude mice and monitored allograft tumor growth over time. Tumor volume continuously increased for *MYCN+;Rb1*$^{f/f Cre}$ allografts (n=20) from week 3 to 6 while *MYCN+*^{Cre} allografts (n=5) grew at a significantly slower rate which also translated to a significant difference in tumor weights between the groups (p=0.0003). Moreover, *MYCN+;Rb1*$^{f/f Cre}$ allograft tumors manifested a similar breakdown and proportion of the different histological patterns to what was observed in primary tumors of *MYCN+;Rb*$^{f/f}$ mice (e.g. AR-positive adenocarcinoma and AR-negative, poorly differentiated foci). Interestingly, allografts from either genotype contained tumor cells that were either AR-negative, weak, or strong, indicating that organoids that were initially AR-positive *in vitro* gradually lost AR expression *in vivo*. However, we observed poorly differentiated foci with NEPC morphology primarily in *MYCN+;Rb1*$^{f/f Cre}$ allografts *MYCN+;Rb1*$^{f/f Cre}$ allograft growth rate was slightly reduced following castration which is likely due to the fact that the tumors were heterogeneous with a component of AR-responsive adenocarcinoma.

Lastly, lung and lymph node metastatic lesions were only observed in mice bearing *MYCN+;Rb1*$^{f/f}$-Cre allografts (**Figure 2H)**. The majority of metastatic lesions were poorly differentiated although some had squamous and osteoid differentiation. Altogether, these data suggest that *MYCN+;Rb1* loss-induced NEPC morphology, loss of AR expression, and increased metastatic potential are independent of the prostate microenvironment.

N-Myc and *Rb1* genomic loss drives a molecular program consistent with NEPC.

To determine if *MYCN* expression synergizes with *Rb1* loss to drive a molecular program associated with NEPC, we performed RNA-seq on histologically distinct tumor foci ranging from adenocarcinoma to NEPC (**Figure 3A**). Previous studies showed that *TP53* mutations can synergize with *RB1* loss to drive a phenotype similar to what we observed in the *MYCN+;Rb1*$^{f/f}$ mice [5,6,10].Therefore, we first queried our RNA-seq data for spontaneous mutations in *Trp53* and in *Rb1.* All single nucleotide variants (SNVs) and insertions/deletions (indels) in the *Trp53* and *Rb1* genes were profiled for each histopathological subtypes of mouse tumors across all genotypes (**Figure 3B**). We observed exonic non-silent mutations in *Trp53* exons and synonymous exonic mutations in *Rb1*. Of the *Trp53* alterations, we noted a missense mutation (c.T715G) in exon 7 within the DNA binding domain. This mutation is equivalent to C242R in the human *TP53* gene (obtained from Vista-Point tool [11,12]) and was found to have a moderate effect (Ensembl Variant Effect Predictor) to deleterious (SIFT) or damaging (PolyPhen) [13,14] impact on TP53 function. The other *Trp53* mutation (c.157dupT) was a frameshift insertion in exon 4 in the linker domain and the human equivalent (W53Cfs*4) was observed to have high impact on TP53 function (Ensembl Variant Effect Predictor). Both human mutations were found in the COSMIC database of mutations, however, none of the observed variants in either gene were specific for poorly differentiated or NEPC tumors in mice irrespective of genotype.

A previously described NEPC score estimates the likelihood a test sample is clinical NEPC based on a set of 70 differentially expressed NEPC-related genes [15]. We calculated the NEPC score for each tumor focus and found that adenocarcinoma foci did not score significantly different from wild type prostates (data not shown). Furthermore, poorly differentiated tumor foci had significantly higher NEPC scores compared to conventional adenocarcinoma and were similar to values obtained from a cohort of patient NEPC tumors ($p < 0.0001$, **Figure 3C**). Interestingly, tumor foci with divergent differentiation (squamous, poor, osteoid) from castrated mice also had NEPC scores similar to clinical NEPC and were significantly higher than adenocarcinoma of intact tumors (p=0.0034). This suggests that castration results in the activation of an NEPC molecular program regardless of histology.

We then compared the expression differences between distinct histological tumor foci to identify differentially expressed pathways associated with accelerated tumor progression. Ward's hierarchal clustering was performed using a 2,043 gene signature that distinguished *MYCN+;Rb1*$^{f/f}$ poorly differentiated/NEPC foci from *MYCN*+ adenocarcinoma foci (adj. $p<0.05$, $|(Log_2 (Fold\ Change)| > 2$), which revealed three distinct sets of gene clusters (**Figure 3D)**. Genes found in clusters 1 and 2 were highly upregulated in poorly differentiated and NEPC-like samples and were enriched with E2F and MYC targets, PRC2 complex, cell cycle, neural lineage and EMT genes (**Figure 3E, F**). Adenocarcinoma foci were enriched with EMT, PRC2 complex and AR signaling/prostate developmental genes. Interestingly, we observed an enrichment of a loss TP53 signaling in poorly differentiated tumor foci compared to adenocarcinoma despite no distinguishing loss of function mutations or change in *Trp53* expression (**Figure 3B**).

3. Specific Aim 3: Determine the impact of the timing of N-Myc on response to NEPC directed therapeutics.

Single Cell-Based Approaches Reveal NEPC-Like Subpopulations.

We next sought to characterize the temporal evolution of tumors in *Rb1*$^{f/f}$ and *MYCN+;R1b*$^{f/f}$ mice. To this end, we performed IHC staining on prostate tissues from 8-week old mice and found that while prostates from *Rb1*$^{f/f}$ mice were composed of AR-positive, HGPIN lesions, tumors from *MYCN+;Rb1*$^{f/f}$ mice contained large regions of AR-positive adenocarcinoma as well as neighboring foci comprised of AR-negative, INSM1-positive cells (**Figure 4A**). In order to better understand this heterogeneity we observed in the developing tumors, we performed single cell RNA sequencing (scRNA-seq) on prostates collected from 8-week old *MYCN+;Rb1*$^{f/f}$ mice as well as age-matched *Rb1*$^{f/f}$ mice and sought to identify subpopulations that may contribute to tumorigenesis. K-means clustering and UMAP projection of the combined data across both genotypes revealed 10 major cell clusters of gene expression (**Figure 4B**). Differential expression analysis between clusters produced a list of the top 50 most differentially expressed genes by cluster (**Figure 4C**), and we assigned identities to each cluster using the expression of known markers (**Figure 4B**). We restricted further analyses to include populations which were identified as luminal epithelium, basal epithelium or neuroendocrine cells on the basis of *Krt5, Krt8, Cd24a, Trp63,* and *Insm1* expression. Re-clustering of this subset allowed for further delineation of the heterogeneity within these populations (*Rb1*$^{f/f}$ mice: 8,151 cells; *MYCN+;Rb1*$^{f/f}$ mice: 5,160 cells) (**Figure 4D**). We then assessed what proportion of each cluster was comprised of cells from each genotype and found striking differences in composition (**Figure 4E**). Using gene expression, we identified a population of cells in *Rb1*$^{f/f}$ tumors that were positive for the luminal markers *Ar* and *Cd24a* as well as had high levels of AR signaling activity assessed by *Fkbp5* expression (**Figure 4F**). This population was markedly reduced in *MYCN+;Rb1*$^{f/f}$ tumors and instead there was an abundance of cells that expressed *Ezh2* and had low levels of AR signaling activity, suggesting a transition away from an AR-dependent state (**Figure 4F**). These data are consistent with previous findings that have shown that N-Myc and EZH2 cooperate to suppress AR signaling [2,3]. Furthermore, the *Ezh2*-positive/AR-signaling low population also had increased expression of a previously published adult stem cell (ASC) signature score [16] and expression of *Sox2*, consistent with the transition away from an adenocarcinoma state (**Figure 4F**). Interestingly, we also identified a population of cells which expressed a number of known neuroendocrine markers, including *Ascl1*, *Chga*, *Foxa2*, and *Insm1* (**Figure 4F**). The ASC signature score was significantly higher in *MYCN+;Rb1*$^{f/f}$ tumors compared to *Rb1*$^{f/f}$ tumors (**Figure 4G**) and was found to be enriched in the cluster containing neuroendocrine cells (**Figure 4H**).

Cell Trajectories Towards a Neuroendocrine-Like Lineage.

In order to understand the transcriptional relationships between the epithelial and neuroendocrine cell populations, we employed a computational method (Monocle) [17] to define cell trajectories between the given lineage states. Clustering of the cells derived from *MYCN+;Rb1*$^{f/f}$ tumors alone again revealed three distinct cell populations consisting of basal and luminal epithelium as well as a neuroendocrine population on the basis of *Krt5, Krt8, Cd24a, Trp63,* and *Insm1* expression (**Figure 5A**). Cell trajectories and UMAP projections highlighted the existence of a transition between luminal epithelial cells and neuroendocrine cells (**Figure 5B**). This was further confirmed by assessing the expression of known marker genes as a function of pseudotime distance from the neuroendocrine population. Keratin 5 (*Krt5*), a known basal epithelial cell marker, was highly expressed in cells with the greatest pseudotime distance from the neuroendocrine population and was largely restricted to the basal epithelial cell population (**Figure 5C**). Levels of *Ar* and its target gene *Tmprss2* were highly expressed in luminal and basal populations and showed low levels of expression in the neuroendocrine population (**Figure 5C**). Robust levels of *Ezh2* were observed throughout all cells, with a modest increase of expression in the neuroendocrine population (**Figure 5C**). As expected, neuroendocrine markers such as *Ascl1*, *Insm1*, *Foxa2*, and *Chga* were all highly expressed in the neuroendocrine population (**Figure 5C**). Surprisingly, this analysis revealed small populations of cells in the luminal epithelial cluster which were beginning to express these neuroendocrine markers, despite being a significant pseudotime distance away from the neuroendocrine population (**Figure 5C**). While the terminal neuroendocrine state also existed in *Rb1*$^{f/f}$ tumors, the appearance of these early-transition cells occurred with higher frequency and at an earlier point in pseudotime in *MYCN+;Rb1*$^{f/f}$ tumors and suggests that this approach can potentially identify cells early in a transition to a neuroendocrine state (**Figure 5C**). We then took an unbiased approach to identify gene modules which were differentially expressed as a function of pseudotime. We identified 22 modules whose expression levels correlated with the three cell states (**Figure 5D**). GSEA performed on the genes from the most highly expressed module in each cluster revealed differences between the clusters, most notably including enrichment of EZH2-related developmental and neural gene sets in the neuroendocrine cluster (cluster 3, **Figure 5E**). The projection of the expression score of the three most highly expressed modules corresponded, as expected, to the three cell states on which they were defined (**Figure 5F**). Intriguingly, while modules 9 and 20 were fairly restricted to luminal and basal populations respectively, module 19 was highly expressed in the neuroendocrine cells as well as a subset of luminal cells that were closest to the neuroendocrine population on the computed cell trajectory (**Figure 5F**). The corresponding module in *Rb1*$^{f/f}$ tumors, while able to identify the neuroendocrine population, did not show a marked enrichment in the cells contained in the luminal population that were along the computed cell trajectory (**Figure 5**).

To better understand the evolution of the cells expressing neuroendocrine markers, we performed scRNA-seq at an earlier time point (6 weeks of age). At this age, prostates of *MYCN+;Rb1*$^{f/f}$ mice contained primarily HGPIN as well as foci of AR-/INSM1- invasive carcinoma .Based on a combined analysis of luminal and neuroendocrine cells in the 6- and 8-week scRNA-seq data, we uncovered two distinct clusters of cells that were AR negative and displayed intermediate to high levels of neuroendocrine marker gene expression (*Insm1*) as well as ubiquitin C-terminal hydrolase L1 (*Uchl1*) (**Figure 5G**). Moreover, these two populations were distinguished by differential expression of *Ascl1/Chga* versus the Oct11-encoding gene *Pou2f3* that is also overexpressed in a subset of clinical CRPC and NEPC tumors (**Figure 5G**). These populations were observed in both 6-week and 8-week timepoints and the cells from both timepoints contributed to all clusters. We next sought to identify genes that marked the intermediate population of cells that were transitioning towards a neuroendocrine phenotype. We performed a differential expression analysis and identified 1,822 genes which were significantly enriched in the cluster of cells found between the luminal and neuroendocrine populations, including *Pou2f3*, *Ovol3*, and *Ascl2* (**Figure 5**).

To determine the clinical relevance of these findings, we performed similar scRNA-seq based approaches on a clinical sample isolated from a patient of Dr. Beltran who presented with an AR-positive prostate adenocarcinoma and AR-negative NEPC liver metastasis. Genomic profiling of the primary tumor identified a 5.8Mb focal deletion of *PTEN* (10:89,536,129-90,122,394) and missense mutation in *TP53* (R273C). While the NEPC liver metastasis shared the *PTEN* deletion with the primary tumor and also harbored a missense mutation in *TP53* (R114C), the metastatic lesion carried a nonsense mutation and predicted loss-of-function of *RB1* (R579X) .The patient progressed following androgen deprivation therapy, docetaxel, and carboplatin treatment and developed an NEPC pleural effusion that was isolated and subjected to scRNA-seq. Analysis of the scRNA-seq data revealed numerous subclusters within the main tumor cell population after removal of hematopoietic and stromal populations (**Figure 5H**). Gene Ontology analysis of the differentially expressed genes between the clusters revealed populations that were enriched for varying cellular processes, including DNA damage response and neural lineage pathways. Similar to the genetic context of the mouse models, the NEPC patient sample contained a substantial number of *MYCN*-positive/*RB1*-negative cells (**Figure 5H**). We also observed a high number of *EZH2*+/AR signaling low cells (**Figure 5H**), many of which also expressed *SOX2* (**Figure 5H**) and *UCHL1*, consistent with our findings in *MYCN+;Rb1*$^{f/f}$ mice. Finally, application of the ASC signature score [16] revealed a strong overlap with cells positive for the marker *MKI67,* indicating the enhanced proliferative capacity of this population . We also performed scRNA-seq on a second prostate cancer sample from a patient who developed a local recurrence in the prostate with mixed small cell carcinoma and adenocarcinoma following ADT treatment. Consistent with our findings in *MYCN+;Rb1*$^{f/f}$ mice, we found a cluster of cells which were strongly positive for the neuroendocrine marker genes *INSM1* and *CHGA* as well as *SOX2* and *UCHL1* in addition to a large cluster of cells which showed marked reduced expression of these genes. RNA velocity analysis of these two populations revealed the existence of cell trajectories which would suggest that cells would most likely transition towards the neuroendocrine cluster.

Distinct Chromatin Accessibility Patterns Exist in Neuroendocrine Subpopulations.

Based on the transcriptional heterogeneity observed during tumorigenesis and the existence of cell trajectories that suggested lineage plasticity between luminal epithelium and neuroendocrine cells, we sought to identify the factors that may be responsible for promoting this change in lineage state. To this end, we performed single cell assay for transposase-accessible chromatin followed by sequencing (scATAC-seq) to determine regions of differential chromatin accessibility between populations. Following library generation and sequencing, fragment sizes varied with a periodicity roughly corresponding to nucleosome spacing (**Figure 6A**). As expected, regions with the highest levels of accessibility were centered around the transcription start site (TSS) of genes (**Figure 6B**). After clustering the chromatin accessibility data, we assessed accessibility at a number of lineage-specific loci (such as *Krt8*, *Psca*, *Ascl1*, *Ptprc*, *Col3a1*, and *Pecam1*) to assign identities (luminal, basal, neuroendocrine, stroma) to the cells. Moreover, we observed distinct subclusters among the basal, luminal, and neuroendocrine populations (**Figure 6C**). The two neuroendocrine subclusters demonstrated high accessibility at known neuroendocrine marker gene loci, therefore we performed a differential accessibility analysis between the NE1 and NE2 populations to uncover differences between these two cluste. From this comparison, we found that the NE1 population had an enrichment of chromatin accessibility at the *Foxa2* locus while the NE2 population had a significant enrichment at the *Ascl2* and *Pou2f3* loci (**Figure 6D**), similar to the scRNA-seq data (**Figure 5G**). In contrast, the genomic loci for *Ar* and the AR target gene *Tmprss2* showed high levels of accessibility in all luminal and basal populations and virtually no accessibility in either of the neuroendocrine populations (**Figure 6D**). We identified regions of chromatin with differential accessibility between all the subpopulations and performed motif analyses to determine the transcription factor binding sites which were

enriched in the hyper-accessible and hypo-accessible regions. As expected, luminal populations were enriched for GATA motifs along with glucocorticoid response elements (GRE) and androgen response elements (ARE) (**Figure 6E**). Interestingly, the neuroendocrine populations were characterized by differential enrichment of ASCL1 motifs in the NE1 population and of OCT/POU family members in the NE2 population (**Figure 6E**), consistent with differences seen in accessibility at the *Pou2f3* loci (**Figure 6D**). In agreement with our scRNA-seq findings, these data suggest the existence of discrete neuroendocrine populations which may be driven by distinct transcriptional programs.

The N-Myc Cistrome Is Altered Upon *Rb1* Loss.

Based on single-cell based sequencing data from the GEMs, we observed that the overexpression of *MYCN* in combination with the loss of *Rb1* resulted in the rapid formation of aggressive, metastatic tumors with neuroendocrine-like features. Thus, we hypothesized that the loss of *Rb1* would synergize with *MYCN* overexpression to reshape the N-Myc cistrome and drive tumor progression. To address this, we performed N-Myc chromatin immunoprecipitation sequencing (ChIP-seq) on multiple, independent tumors collected from *MYCN*+ or *MYCN+;Rb1*$^{f/f}$ mice. Consistent with its role as a transcription factor, N-Myc binding was highly enriched near the transcription start site (TSS) of genes in both genotypes. We found 36,789 N-Myc peaks in *MYCN*+ tumors, in relative agreement with our previous studies of N-Myc binding in human prostate cancer cells [2]. Surprisingly, following the loss of *Rb1*, the N-Myc cistrome was dramatically expanded to 62,171 binding sites with nearly 60% of these sites corresponding to new binding sites not seen in *MYCN*+ mice alone (**Figure 7A**). Additionally, GSEA of the *MYCN*+ and *MYCN+;Rb1*$^{f/f}$ unique peaks revealed distinct sets of genes bound by N-Myc between the conditions. While many luminal epithelial and hormone-responsive gene sets were enriched in *MYCN*+ tumors, a large enrichment of PRC2 complex targets, epigenetically marked developmental, and neural lineage gene sets was found in *MYCN+;Rb1*$^{f/f}$ tumors. To determine the transcriptional co-factors which may contribute to this differentially remodeled cistrome, we performed motif enrichment analysis between N-Myc peaks unique to the *MYCN*+ and *MYCN+;Rb1*$^{f/f}$ mice. While the most differentially enriched motifs in *MYCN*+ tumors consisted of TP53 and ARE motifs, *MYCN+;Rb1*$^{f/f}$ tumors were enriched for ASCL and SNAIL family motifs (**Figure 7B**). More strikingly, a high degree of enrichment was observed for a motif consistent with the E2F family of transcription factors [18] (**Figure 7B**). To assess the degree of altered N-Myc binding and chromatin accessibility, we integrated the scATAC-seq and the ChIP-seq data and restricted the analysis to regions of differential accessibility between subpopulations. In the presence of wild-type levels of *Rb1*, N-Myc was bound at regions of accessible chromatin associated with luminal populations (**Figure 7C**). In the context of *Rb1* loss, N-Myc binding was reduced in the luminal-specific regions and instead was dramatically enriched in regions which were accessible only in the neuroendocrine populations (**Figure 7C**). Specifically, we found that N-Myc binding was reduced at the *Ar* locus and redirected to neuroendocrine-associated genes, such as *Ascl1* and *Insm1*, in *MYCN+;Rb1*$^{f/f}$ tumors (**Figure 7D**). Importantly, the loss of *Rb1* appeared to remodel the N-Myc cistrome in a very specific manner, as binding at the *Gapdh* locus (a known N-Myc target gene) remained consistent between *MYCN*+ and *MYCN+;Rb1*$^{f/f}$ tumors (**Figure 7D**). Together, these data suggest that the loss of *Rb1* synergizes with N-Myc overexpression to redirect the N-Myc cistrome to new genomic loci to regulate gene expression, possibly with the help of ASCL- and E2F-family members.

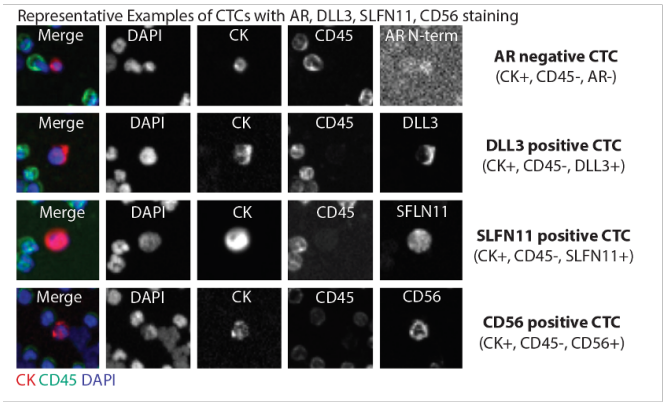

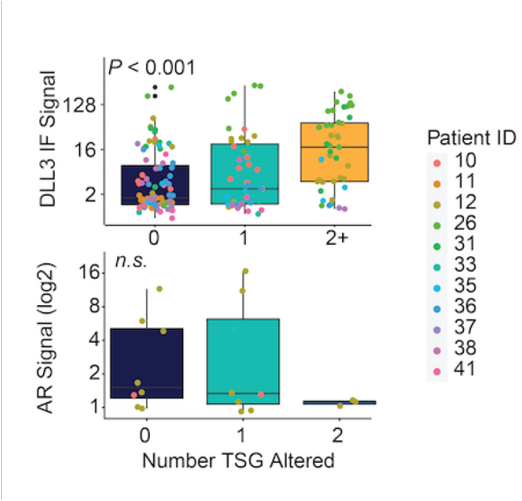

Figure 1. A) Representative images of CK+, CD45- CTCs detected in NEPC with small-cell like features (N/C ratio greater than 0.8 and area less than approximately 2x that of white blood cells. CTCs stained with a 4th marker for AR, DLL3, SLFN11, or CD56. In the three-color composite image, blue represents 4′,6-diamidino-2-phenylindole (DAPI), and red is used for CK, green for CD45, and white for DLL3. B) **C)** Intensity of DLL3 or AR protein expression in 199 CTCs collected from 12 patients with NEPC and CRPC assessed by immunofluorescence compared tumor suppressor loss (PTEN, RB1, P53) in single CTCs.

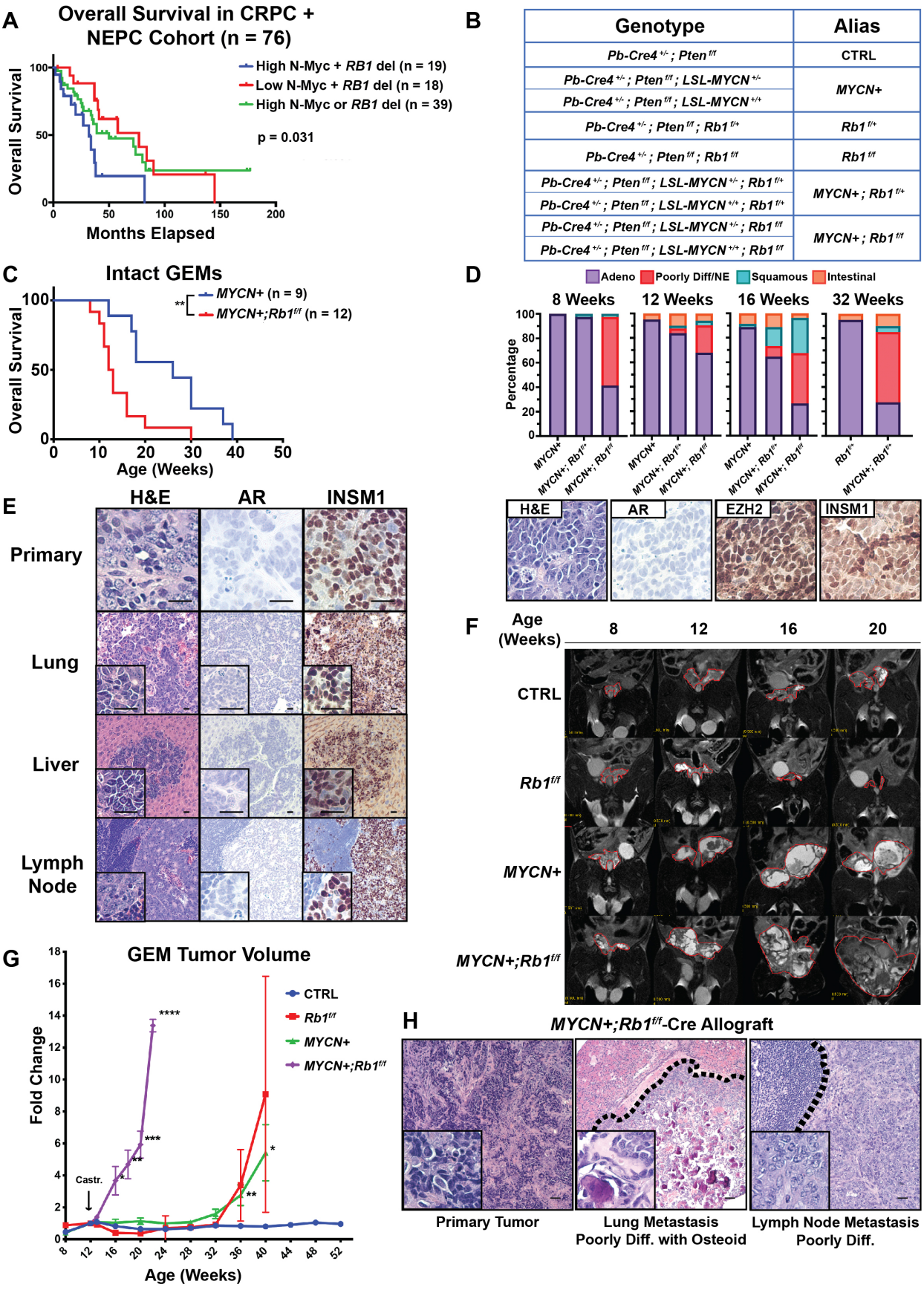
A
Overall Survival in CRPC + NEPC Cohort (n = 76)
High N-Myc + RB1 del (n = 19)
Low N-Myc + RB1 del (n = 18)
High N-Myc or RB1 del (n = 39)
p = 0.031
Overall Survival
Months Elapsed
B
Genotype
Alias
Pb-Cre4 +/- ; Pten f/f
CTRL
Pb-Cre4 +/- ; Pten f/f ; LSL-MYCN +/-
Pb-Cre4 +/- ; Pten f/f ; LSL-MYCN +/+
MYCN+
Pb-Cre4 +/- ; Pten f/f ; Rb1 f/+
Rb1 f/+
Pb-Cre4 +/- ; Pten f/f ; Rb1 f/f
Rb1 f/f
Pb-Cre4 +/- ; Pten f/f ; LSL-MYCN +/- ; Rb1 f/+
Pb-Cre4 +/- ; Pten f/f ; LSL-MYCN +/+ ; Rb1 f/+
MYCN+ ; Rb1 f/+
Pb-Cre4 +/- ; Pten f/f ; LSL-MYCN +/- ; Rb1 f/f
Pb-Cre4 +/- ; Pten f/f ; LSL-MYCN +/+ ; Rb1 f/f
MYCN+ ; Rb1 f/f
C
Intact GEMs
MYCN+ (n = 9)
MYCN+;Rb1f/f (n = 12)
**
Overall Survival
Age (Weeks)
D
Adeno
Poorly Diff/NE
Squamous
Intestinal
8 Weeks
12 Weeks
16 Weeks
32 Weeks
Percentage
MYCN+
MYCN+; Rb1f/+
MYCN+; Rb1f/f
Rb1f/+
MYCN+; Rb1f/+
H&E
AR
EZH2
INSM1
E
H&E
AR
INSM1
Primary
Lung
Liver
Lymph Node
F
Age (Weeks)
8
12
16
20
CTRL
Rb1f/f
MYCN+
MYCN+;Rb1f/f
G
GEM Tumor Volume
CTRL
Rb1f/f
MYCN+
MYCN+;Rb1f/f
Fold Change
Castr.
Age (Weeks)
H
MYCN+;Rb1f/f-Cre Allograft
Primary Tumor
Lung Metastasis
Poorly Diff. with Osteoid
Lymph Node Metastasis
Poorly Diff.

Figure 2. *MYCN*+ and *RB1* deletion accelerates progression to NEPC. A. Kaplan-Meier plots of CRPC (n=55) and NEPC (n=21) patients stratified into three categories according *MYCN* (N-Myc) expression and/or *RB1* status. Univariate overall survival analysis was calculated from the time of initial diagnosis of metastatic disease to death from any cause. Patients still alive at time of last follow-up were censored. Patients with high N-Myc expression and *RB1* deletion showed significantly worse survival compared to the other two groups (p=0.031, Kaplan-Meier estimator (log-rank test). **B.** Table of genotype aliases used. **C.** Survival plots of intact *MYCN*+ or *MYCN*+;*Rb1*$^{f/f}$ mice using the Kaplan-Meier estimator (log-rank test). **D.** Top: percentage of GEM tumor foci with conventional adenocarcinoma (including HGPIN, intracystic carcinoma, adenocarcinoma), poorly differentiated/neuroendocrine features, squamous differentiation, and intestinal differentiation based on pathologist assessment. Bottom: Hematoxylin and eosin (H&E) and IHC staining of NEPC focus for N-Myc, RB1, epithelial markers AR and CK8, reprogramming factor EZH2, and small cell neuroendocrine marker INSM1. Scale bar: 50 μm. **E.** H&E and IHC of AR, N-Myc, INSM1 on primary tumor, lung, liver, and lymph node metastasis in a *PbCre*$^{+/-}$; *Pten*$^{f/+}$; *MYCN*$^{+/+}$; *Rb1*$^{f/f}$ 19-week-old mouse. Scale bar: 50 μm. **EF** MRI coronal scans from CTRL (n=5), *Rb1*$^{f/f}$ (n=3); *MYCN*+ (n=4); and *MYCN*+;*Rb1*$^{f/f}$ (n=6) GEMs from 8 to 20 weeks of age. Mice were castrated at 12 weeks of age. **G.** Fold change volume over time of GEM tumors from mice castrated at 12 weeks. *p<0.05, **p<0.01, ***p<0.001, ****p<0.0001. **H.** H&Es of poorly differentiated subcutaneous mouse allograft primary tumor and metastases derived from Adeno-Cre-transduced *MYCN*+;*Rb1*$^{f/f}$ organoids. The dashed lines separate the tumor metastasis from normal tissue. Scale bar: 50 μm.

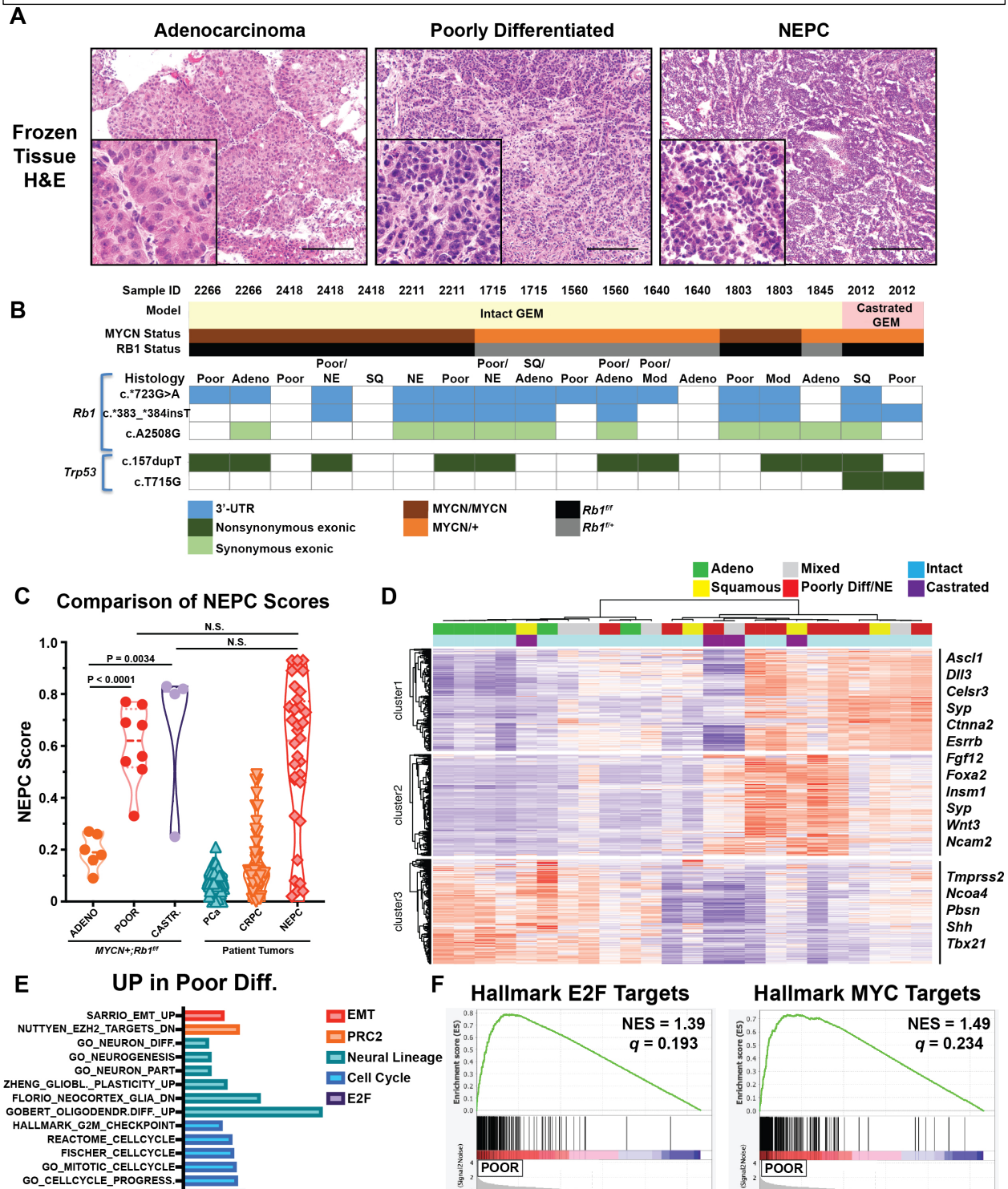

Figure 3. Poorly differentiated tumors have molecular signatures similar to clinical NEPC. A. H&E from frozen tumors showing examples of adenocarcinoma, poorly differentiated, and NEPC histology. Scale bar: 50 μm. **B.** Single nucleotide variants and indels at *Trp53* and *Rb1* in mouse tumors from RNA-seq data. **C.** Left: Violin plot of NEPC scores from *MYCN+;Rb1*$^{f/f}$ GEMs with conventional adenocarcinoma and poorly differentiated/NEPC histologies, as well as PCa, CRPC, and NEPC patient samples. **D.** Heatmap and hierarchal clustering of poor, squamous, adenocarcinoma and mixed differentiation foci from GEMs based on the *MYCN+;Rb1*$^{f/f}$ POOR vs. *MYCN+* ADENO Signature. **E.** Top gene sets related to E2F targets, cell cycle, neuronal development, epigenetic reprogramming, epithelial identity, p53 targets, and AR signaling. UP: log2FC > 1.5 DOWN: log2FC < -1.5, p < 0.05. **F.** GSEA enrichment plots of Hallmark E2F Targets and Hallmark MYC Targets in poorly differentiated (POOR) vs. adenocarcinoma (ADENO).

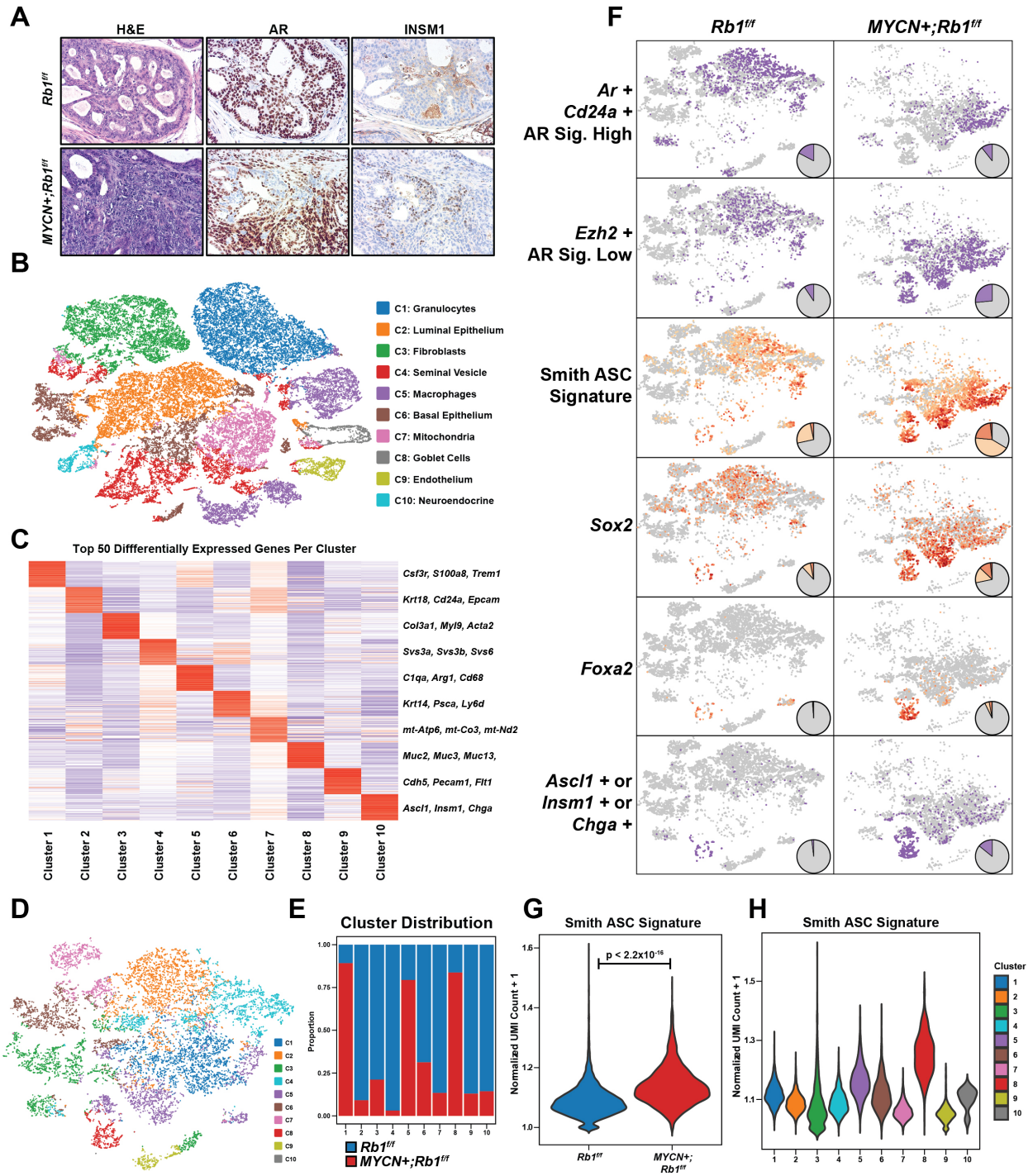

Figure 4. Single cell-based approaches reveal NEPC-like subpopulations. A. H&E and IHC staining of AR and INSM1 in samples used for scRNA-seq. **B.** Combined t-SNE plot of scRNA-seq data from *Rb1*$^{f/f}$ (n=3) and *MYCN+;Rb1*$^{f/f}$ (n=3) mice. **C.** Clustering of the top 50 most differentially expressed genes between clusters. **D.** Reclustering of combined luminal, basal and neuroendocrine

populations from *Rb1*$^{f/f}$ (n=3) and *MYCN+;Rb1*$^{f/f}$ (n=3) mice. **E.** Distribution of genotypes between clusters identified in panel D. **F.** Expression of indicated markers or signature in *Rb1*$^{f/f}$ (n=3) compared to *MYCN+;Rb1*$^{f/f}$ (n=3) mice. Pie charts show proportions of positive vs. negative cells or high/medium/low/negative gene expression. **G.** Violin plot of Smith ASC score [16]. **H.** ASC score by cluster from panel D.

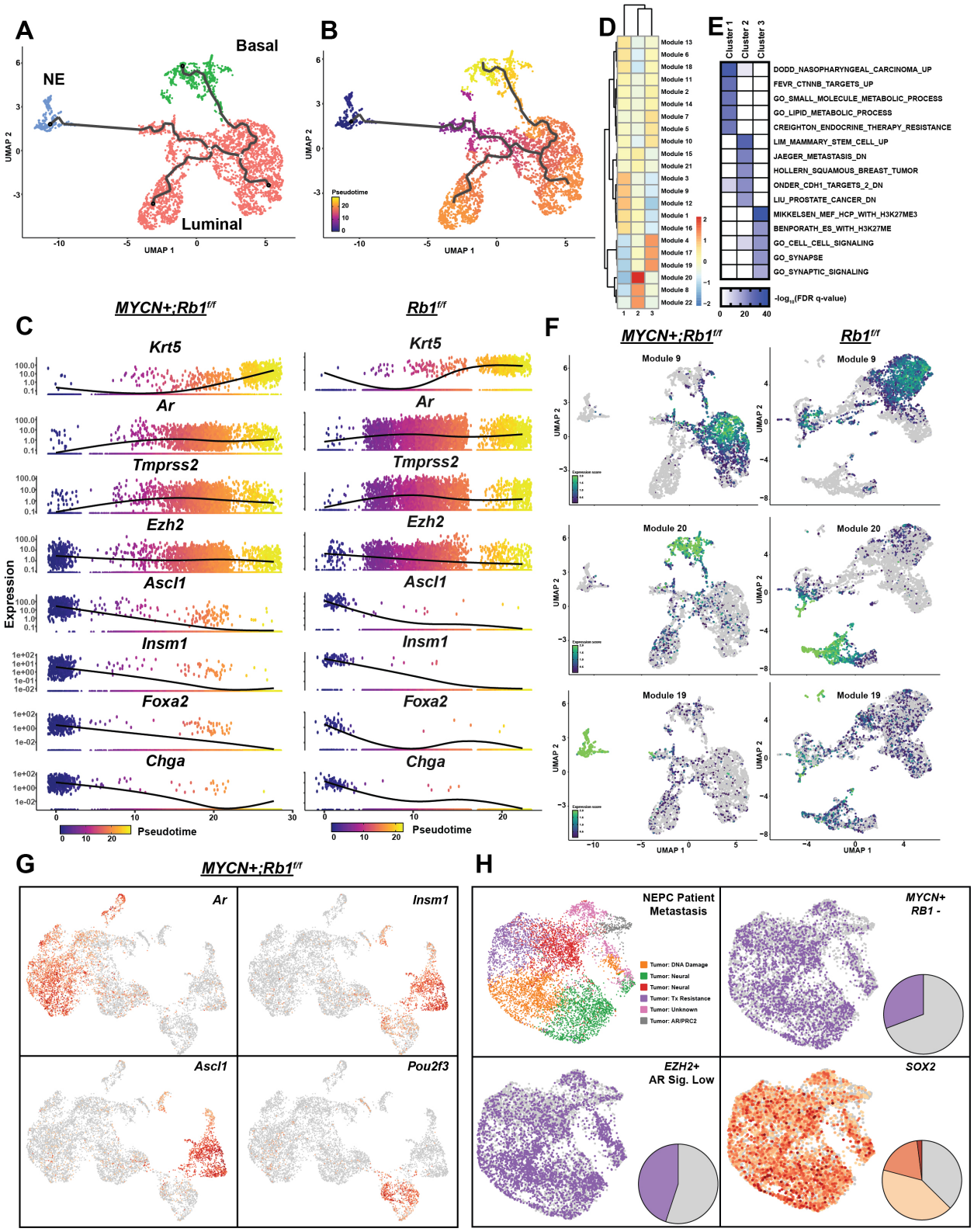

Figure 5. Cell trajectories towards a neuroendocrine-like lineage. A. t-SNE projection of luminal (red), basal (green), and neuroendocrine (blue) populations from *MYCN+;Rb1*$^{f/f}$ mice (n=3). **B.** Pseudotime trajectories projected onto t-SNE from panel A. **C.** Gene expression levels of indicated genes over pseudotime (neuroendocrine population located at t=0) in *MYCN+;Rb1*$^{f/f}$ (left) and *Rb1*$^{f/f}$ (right) mice. **D.** Heatmap and clustering of gene expression modules which vary significantly as a function of pseudotime in *MYCN+;Rb1*$^{f/f}$ mice. **E.** GSEA results showing the top 5 gene set enriched in modules 9, 19, and 20. **F.** Expression of genes from modules 9, 19 and 20 projected onto *MYCN+;Rb1*$^{f/f}$ (left) and *Rb1*$^{f/f}$ (right) mice. **G.** Expression of indicated genes in luminal and neuroendocrine cells of 6-week-old (n=2) and 8-week-old (n=3) *MYCN+;Rb1*$^{f/f}$ mice. **H.** UMAP of scRNA-seq data from a metastatic NEPC sample. Clusters were named based on GSEA results of differentially expressed genes between clusters.

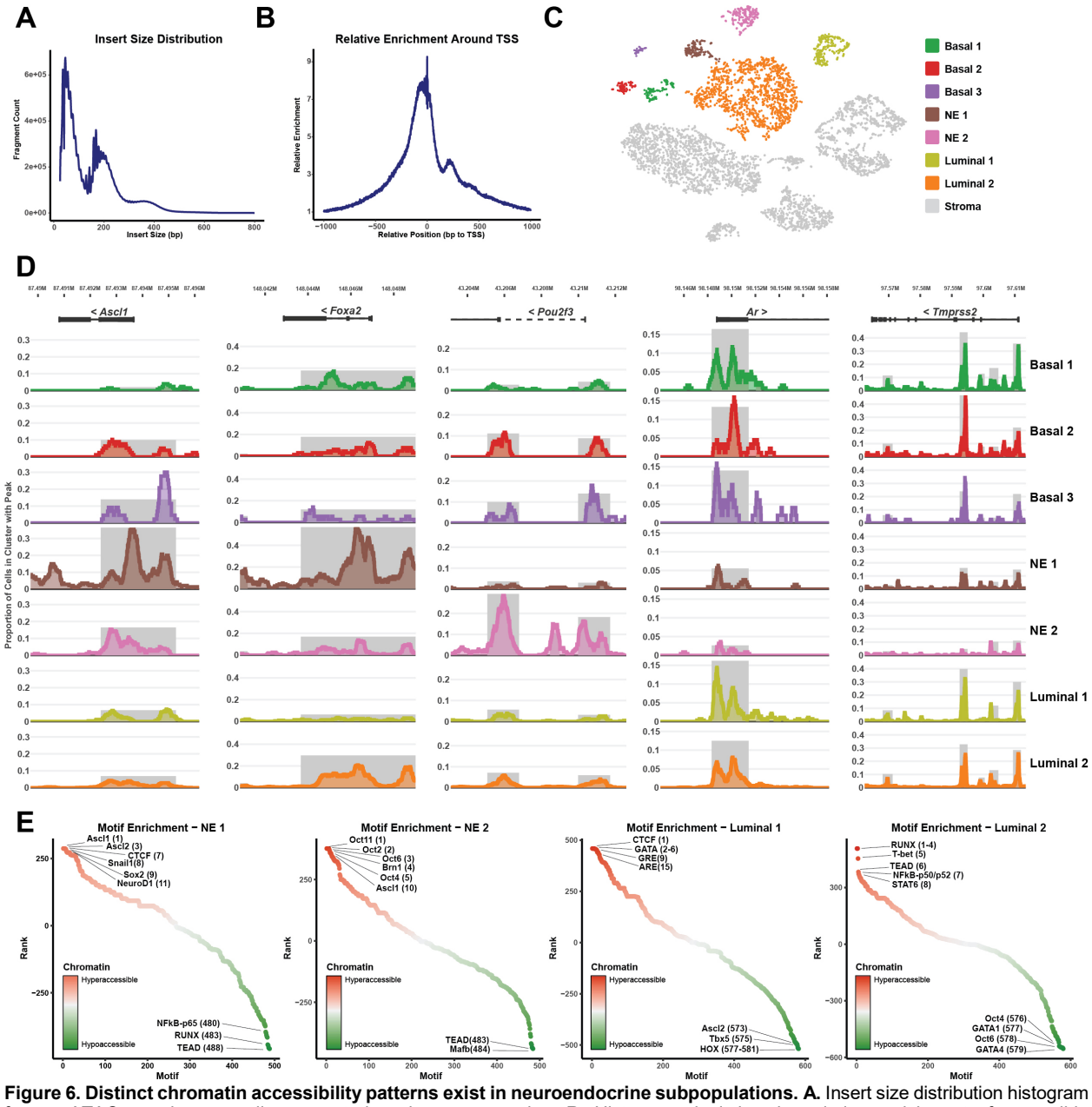

Figure 6. Distinct chromatin accessibility patterns exist in neuroendocrine subpopulations. A. Insert size distribution histogram from scATAC-seq data revealing expected nucleosome spacing. **B.** Histogram depicting the relative enrichment of accessible chromatin centered at the transcription start site (TSS) of genes. **C.** t-SNE plot of scATAC-seq data from *MYCN+;Rb1*$^{f/f}$ mice. **D.** Chromatin accessibility in the subpopulations at the indicated loci. **E.** Graphs of differential transcription factor motif enrichment in the indicated subpopulations called on regions of hyper- and hypo-accessible chromatin between clusters.

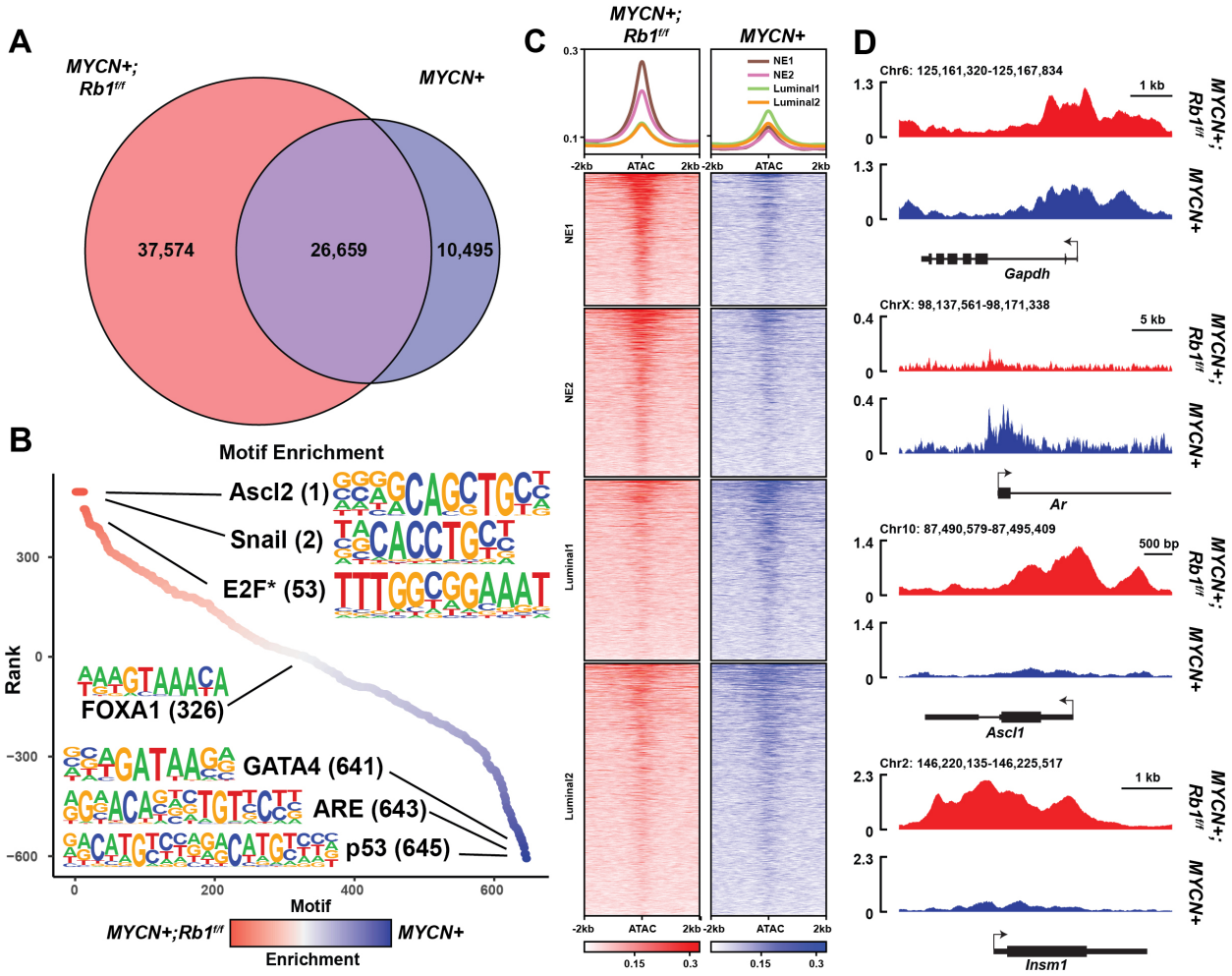

Figure 7. The N-Myc cistrome is altered upon Rb1 loss. A. Venn diagram showing the overlap of N-Myc binding by ChIP-seq from *MYCN+;Rb1*$^{f/f}$ (n=3) and *MYCN+* (n=2) tumors (peak cutoff: q < 0.0001). **B.** Differential transcription factor motif enrichment between N-Myc binding sites in *MYCN+;Rb1*$^{f/f}$ and *MYCN+* tumors. **C.** Heatmaps of N-Myc binding in *MYCN+;Rb1*$^{f/f}$ and *MYCN+* tumors at regions of accessible chromatin associated with neuroendocrine and luminal subpopulations by scATAC-seq in Figure 5C. **D.** N-Myc binding at indicated loci in *MYCN+;Rb1*$^{f/f}$ (n=3) and *MYCN+* (n=2) tumors.

What opportunities for training and professional development has the project provided?

Presentations:

- Prostate Cancer Foundation, Carlsbad, CA.
  Annual Scientific Retreat
- Society for Basic Urologic Research, New Orleans, LA.
  Annual Scientific Retreat
- WCM BCMB Graduate School Retreat, New Paltz, NY
- New York Prostate Club Meeting, New York, NY
  Quarterly meeting of prostate cancer researchers from Weill Cornell Medicine, MSKCC, Columbia University, and Rockefeller University.
- Multi-Institutional Prostate Cancer Program Retreat, Ft. Lauderdale, FL
  Annual meeting of institutions with an NCI-funded P50 SPORE grant in prostate cancer research. poster was selected for an oral presentation and was awarded first-place in 2020.

Workshops/Training Opportunities:

- Biostatistics Seminar Series (WCM)
  This is a monthly lecture series geared towards clinical investigators, research staff, and students who are interested in gaining insight into fundamental research design and statistical concepts with a focus on practical knowledge.
- Transitioning to Research Independence (WCM/Tri-I)
  A set of seminars to help you attain and maintain a successful career in academic research
- Workshops through Applied Bioinformatics Core (WCM/Tri-I)
  Regularly held, intensive 12-hours-long courses open to members of the Tri-Institutional network
- Trainee Affairs Career Symposium and Networking Dinner, SBUR Meeting
  Focused on career development plans and the nuts and bolts of setting up and running a research lab
- *Ad hoc* reviewer for Cancer Cell, Molecular Cell, Nature Communications, *Cell Reports* and *Science Translational Medicine*
  Critically reviewed manuscripts for publication in related fields

Drs Beltran and Rickman are fully committed to furthering the training and professional development of the post-doctoral fellows and students affiliated to this project. This has including presentations at PCF, AACR, Prostate Cancer SPORE Retreats, SBUR meetings. The pandemic has prohibited face to face meetings, but we have facilitated opportunities for networking via conference calls and virtual meeting participation. Dr. Nick Brady (postdoctoral fellow in the Rickman lab) received prize for best abstract at the; Prostate Cancer SPORE program Annual Retreat, February 2020. Nick also competed successfully for an American Cancer Society postdoctoral award (awarded Aug 2020). Dr. Richa Singh (Rickman lab) and Dr. Shengyu Ku (Beltran lab) received Department of Defense postdoctoral training awards.

Postdoc fellows also participate in the following:
NIH T32 MTOR Course. 15 lectures, especially designed for MTOR, will be presented by our preceptors jointly with their clinical collaborators to showcase the principles of translational cancer research and team science.

Transitioning to Research Independence seminar series. A seminar series geared towards postdoctoral researchers and fellows who plan to set up their own laboratory and develop their own research program at an academic institution. Trainees will comprehend the faculty application process; understand strategies for funding, mentoring and leadership to effectively run their own research group.

Biostatistics Lecture Series through the Clinical and Translational Science Center. This is a monthly lecture series geared towards clinical investigators, research staff, and students who are interested in gaining insight into fundamental research design and statistical concepts with a focus on practical knowledge.

We presented at the Multi-institutional Prostate Cancer Meeting in Ft Lauderdale in February 2020 which is organized and led by the SPORE programs. The following manuscripts are related to this project:

1. Puca, L., et al., **Nat Commun**, 2018. 9(1): p. 2404.

2. Beltran, H., et al., **Clin Cancer Res**, 2018.

3. Beltran et al. **Clinical Cancer Research** (2019)

4. Puca L... Beltran H, **Science Translational Medicine** (2019)

5. Berger, A., Brady, N … Rickman DS, **Journal of Clinical Investigation** (2019)

6. Beltran et al… **Clinical Cancer Research** (2019)

7. Conteduca V. et al…. Beltran H**. European Journal of Cancer** (2019)

8. Beltran et al… **Journal of Clinical Investigation** (2020)

9. Brady, N., et al. …Beltran, H.,..Rickman, DS *Temporal evolution of cellular heterogeneity during the progression to advanced, AR-negative prostate cancer*, **Nature Communications** (2021)

10. Conteduca et al… Beltran, **NPJ Precision Oncology** (2021)

What do you plan to do during the next reporting period to accomplish the goals?
If this is the final report, state "Nothing to Report."

Related to Aim 1, we continue to recruit patients for this study. We will focus on correlating the signatures obtained from our mouse model (MYCN induction with Pten/Rb1 co-loss) in the tumor specimens) of clinical cohorts including CRPC patients treated with abiraterone or enzalutamide and a cohort of high risk localized prostate cancers from patients enrolled on a Phase 3 trial (NCT00430183) to assess the frequency and clinical impact of N-myc expression with or without tumor suppressor alterations in untreated high risk prostate cancer. We profiled circulating tumor cells (CTCs) from CRPC/NEPC by single-cell whole genome sequencing and immunofluorescence, and will evaluate N-myc expression.

Related to Aim 2, we will continue our analyses of the N-Myc cistrome and how other transcription factors (e.g. ASCL1 and POU2F3) may function to mediate the driving role of N-Myc on the the molecular program associated with NEPC. For this we will rely on our new GEM described above. We will perform genetic experiments (knock-in/knock-out) of specific cofactors to determine their cooperative role with N-Myc in driving this phenotype.

Related to Aim 3, we are developing opportunities for clinical trial development for NEPC, specifically around EZH2 (Daiichi Sankyo).

4. **IMPACT:** Describe distinctive contributions, major accomplishments, innovations, successes, or any change in practice or behavior that has come about as a result of the project relative to:

What was the impact on the development of the principal discipline(s) of the project?
If there is nothing significant to report during this reporting period, state "Nothing to Report."

While *RB1* loss is common in prostate cancer and N-Myc overexpression occurs in a large proportion of NEPC, little is known about the potential synergy between these two events. Here, we have used a cohort of CRPC and NEPC patients, exploring both gene expression and outcomes data, to determine that the co-occurrence of *RB1* loss and N-Myc overexpression is

associated with a worse overall survival than either event alone. To study the mechanism behind this association, we generated a GEM combining dual *Pten* and *Rb1* loss with N-Myc overexpression. These mice rapidly developed tumors with poorly differentiated histology and were significantly more castration-resistant than control animals.

The degree of differences between the transcriptomes of specific histologies (e.g. adenocarcinoma vs. poorly differentiated/NEPC) based on bulk RNA-seq was not surprising given the dramatic phenotypic differences. However, the striking differences in the N-Myc cistrome in the context of Rb1 loss were intriguing and unexpected, and we hypothesized that cofactors and/or other transcription factors could account for these differences. Interestingly, we observed an enrichment of E2F and MYC targets in poorly differentiated tumor foci compared to adenocarcinoma, suggesting that E2F and N-Myc may have altered or enhanced activity in the transition from adenocarcinoma to a poorly differentiated state. This was also reflected in our ChIP-seq studies where E2F motifs were enriched at N-Myc binding sites that were uniquely found in poorly differentiated tumors. For N-Myc, this is consistent with our previous findings that the N-Myc cistrome can be dynamically regulated [2]. However, in the context of androgen withdrawal, N-Myc binding sites were enriched for Forkhead motifs. Interestingly, the FOXA1 motif was equally enriched in both *MYCN+* and *MYCN+;Rb1$^{f/f}$* tumors. Instead, the enrichment of an E2F motif at N-Myc binding sites in the context of *Rb1* loss suggests that N-Myc binds at E2F target genes and synergizes to drive a tumorigenic transcriptional state. Further work is needed to determine if E2F transcription factors cooperate with N-Myc and redirects N-Myc binding in the context of *RB1* loss. Downregulated genes were enriched in epigenetic reprogramming and PRC2 targets, as well as epithelial identity, AR signaling and P53 targets. Our previous work demonstrated that N-Myc activates EZH2 transcriptional reprogramming, which plays an important role in driving neuroendocrine prostate cancer [3]. Enrichment of PRC2 target genes and epigenetically marked genes (H3K27me3, associated with repression) suggests a shift in epigenetic reprogramming mediated by PRC2 when cells transition from adenocarcinoma to a poorly differentiated/NEPC phenotype. We also observed downregulation of genes related to epithelial identity, such as those that are downregulated by loss of epithelial adhesion molecule E-cadherin (CDH1). Loss of E-cadherin is thought to promote metastasis through the initiation of EMT and invasiveness [19]. We primarily saw metastatic lesions with poorly differentiated histology in our GEMs and mouse allografts, suggesting that poorly differentiated cells have higher metastatic potential due to activation of EMT pathways. Interestingly, our use of organoid-derived subcutaneous allografts revealed that the development of NEPC-like disease can occur in the context of *Rb1* loss and N-Myc overexpression independently of the prostate microenvironment. Further studies are needed to fully appreciate the role of the tumor microenvironment in shaping early prostate tumorigenesis.

Using RRBS to query changes in DNA methylation across our *in vivo* and *in vitro* models, as well as patient samples, we found that components of the DNA methylation machinery were deregulated in poorly differentiated/NE tumors compared to adenocarcinomas. This corresponded to differential methylation statuses across a number of clinically relevant loci throughout the genome. Based on our methylation data from GEM tumors, we developed a 360 gene methylation signature which successfully segregated clinical CRPC and NEPC samples. It remains to be seen how levels of DNA methylation track with levels of H3K27me3 and chromatin accessibility.

Given the heterogeneity in the developing tumors, single-cell based approaches allowed for a refined characterization of the oncogenic transformation. Single cell RNA-seq studies recapitulated our previous reports of the role of N-Myc and EZH2 cooperating to suppress AR signaling [2,3]. We have also demonstrated that the population of cells expressing known neuroendocrine markers also showed increased expression of a gene expression signature correlated with poor survival in patients [16]. Of particular note, we found an upregulation of a number of neuroendocrine marker genes in cells that were not part of the distinct neuroendocrine

cluster and were a large distance away in pseudotime. These data strongly support the notion that cells transition from a luminal-like state towards an NEPC-like state and are not simply an expansion of existing neuroendocrine precursor cells. Moreover, as many of these cells expressed AR but had low levels of AR target genes, it suggests that pharmacologic inhibition of EZH2 may restore androgen signaling and reverse the induced NE transcriptional program. This is particularly relevant as a number of clinical trials using EZH2 inhibitors are currently in progress, including many in prostate cancer (NCT03480646, NCT04179864, NCT03460977). Additionally, both our scRNA-seq and scATAC-seq studies found two distinct neuroendocrine clusters on the basis of transcription and chromatin accessibility. These two clusters differed in their expression of *Ascl1 and Pou2f3* as well as in their enrichment for ASCL and POU/OCT transcription factor family binding motifs. Recent work in small cell lung cancer (SCLC) has found Notch activation in c-Myc-driven tumors can promote a switch between ASCL1-positive, NEUROD1-positive, and YAP1-positive states [20]. Our previous studies have shown that, while c-Myc and N-Myc share a number of common target genes, the N-Myc cistrome in prostate cells encompasses a larger and more diverse set of transcriptional targets [2]. We did find enrichment of NeuroD1 motifs in the scATAC-seq data from one of the neuroendocrine subpopulations. It is possible that changes to accessible motifs mark populations that are undergoing a transition between states. Additional work is needed to understand how these two subpopulations are regulated and if there are different lineage outcomes for a cell depending on which of the populations served as cluster of origin.

Altogether, our studies have identified a population of cells which downregulate AR signaling and undergo a lineage transformation to a neuroendocrine-like phenotype following N-Myc over-expression and *Pten/Rb1* co-loss. This lineage change was accompanied by changes in chromatin accessibility and N-Myc binding at a number of clinically relevant genes. Finally, we identified a methylation signature which may inform future clinical trials using EZH2 inhibitors as to which patients are most likely to benefit from EZH2 inhibition and as a biomarker to identify patients who show a beneficial response. These studies have shed light on the molecular mechanisms by which N-Myc overexpression and *Rb1* loss synergize to drive the development of neuroendocrine prostate cancer and have provided new avenues of exploration towards identifying and validating new therapeutic targets.

References

1 Beltran, H. *et al.* Molecular characterization of neuroendocrine prostate cancer and identification of new drug targets. *Cancer Discov* **1**, 487-495, doi:10.1158/2159-8290.CD-11-0130 (2011).

2 Berger, A. *et al.* N-Myc-mediated epigenetic reprogramming drives lineage plasticity in advanced prostate cancer. *J Clin Invest* **130**, 3924-3940, doi:10.1172/JCI127961 (2019).

3 Dardenne, E. *et al.* N-Myc Induces an EZH2-Mediated Transcriptional Program Driving Neuroendocrine Prostate Cancer. *Cancer Cell* **30**, 563-577, doi:10.1016/j.ccell.2016.09.005 (2016).

4 Lee, J. K. *et al.* N-Myc Drives Neuroendocrine Prostate Cancer Initiated from Human Prostate Epithelial Cells. *Cancer Cell* **29**, 536-547, doi:10.1016/j.ccell.2016.03.001 (2016).

5 Ku, S. Y. *et al.* Rb1 and Trp53 cooperate to suppress prostate cancer lineage plasticity, metastasis, and antiandrogen resistance. *Science* **355**, 78-83, doi:10.1126/science.aah4199 (2017).

6 Mu, P. *et al.* SOX2 promotes lineage plasticity and antiandrogen resistance in TP53- and RB1-deficient prostate cancer. *Science* **355**, 84-88, doi:10.1126/science.aah4307 (2017).
7 Balanis, N. G. *et al.* Pan-cancer Convergence to a Small-Cell Neuroendocrine Phenotype that Shares Susceptibilities with Hematological Malignancies. *Cancer Cell* **36**, 17-34 e17, doi:10.1016/j.ccell.2019.06.005 (2019).
8 Rosenbaum, J. N. *et al.* INSM1: A Novel Immunohistochemical and Molecular Marker for Neuroendocrine and Neuroepithelial Neoplasms. *American journal of clinical pathology* **144**, 579-591, doi:10.1309/AJCPGZWXXBSNL4VD (2015).
9 Agoff, S. N. *et al.* Thyroid transcription factor-1 is expressed in extrapulmonary small cell carcinomas but not in other extrapulmonary neuroendocrine tumors. *Mod Pathol* **13**, 238-242 (2000).
10 Zhou, Z. *et al.* Synergy of p53 and Rb deficiency in a conditional mouse model for metastatic prostate cancer. *Cancer Res* **66**, 7889-7898, doi:66/16/7889 [pii]
10.1158/0008-5472.CAN-06-0486 (2006).
11 Dubchak, I. *et al.* Active conservation of noncoding sequences revealed by three-way species comparisons. *Genome Res* **10**, 1304-1306, doi:10.1101/gr.142200 (2000).
12 Frazer, K. A., Pachter, L., Poliakov, A., Rubin, E. M. & Dubchak, I. VISTA: computational tools for comparative genomics. *Nucleic Acids Res* **32**, W273-279, doi:10.1093/nar/gkh458 (2004).
13 Cerami, E. *et al.* The cBio cancer genomics portal: an open platform for exploring multidimensional cancer genomics data. *Cancer Discov* **2**, 401-404, doi:10.1158/2159-8290.CD-12-0095 (2012).
14 Gao, J. *et al.* Integrative analysis of complex cancer genomics and clinical profiles using the cBioPortal. *Sci Signal* **6**, pl1, doi:10.1126/scisignal.2004088 (2013).
15 Beltran, H. *et al.* Divergent clonal evolution of castration-resistant neuroendocrine prostate cancer. *Nat Med* **22**, 298-305, doi:10.1038/nm.4045 (2016).
16 Smith, B. A. *et al.* A Human Adult Stem Cell Signature Marks Aggressive Variants across Epithelial Cancers. *Cell Rep* **24**, 3353-3366 e3355, doi:10.1016/j.celrep.2018.08.062 (2018).
17 Trapnell, C. *et al.* The dynamics and regulators of cell fate decisions are revealed by pseudotemporal ordering of single cells. *Nat Biotechnol* **32**, 381-386, doi:10.1038/nbt.2859 (2014).
18 Korenjak, M., Anderssen, E., Ramaswamy, S., Whetstine, J. R. & Dyson, N. J. RBF binding to both canonical E2F targets and noncanonical targets depends on functional dE2F/dDP complexes. *Mol Cell Biol* **32**, 4375-4387, doi:10.1128/MCB.00536-12 (2012).
19 Onder, T. T. *et al.* Loss of E-cadherin promotes metastasis via multiple downstream transcriptional pathways. *Cancer Res* **68**, 3645-3654, doi:10.1158/0008-5472.CAN-07-2938 (2008).
20 Ireland, A. S. *et al.* MYC Drives Temporal Evolution of Small Cell Lung Cancer Subtypes by Reprogramming Neuroendocrine Fate. *Cancer Cell*, doi:10.1016/j.ccell.2020.05.001 (2020).

What was the impact on other disciplines?
If there is nothing significant to report during this reporting period, state "Nothing to Report."

Describe how the findings, results, or techniques that were developed or improved, or other products from the project made an impact or are likely to make an impact on other disciplines.

Results from this study may provide insights in other cancer types that develop lineage plasticity as a resistance mechanism to targeted therapies (eg., EGFR mutated lung adenocarcinomas that transform to small cell carcinoma), as there are shared molecular features and potentially shared therapeutic implications.

What was the impact on technology transfer?
If there is nothing significant to report during this reporting period, state "Nothing to Report."

Nothing to report.

What was the impact on society beyond science and technology?
If there is nothing significant to report during this reporting period, state "Nothing to Report."

Describe how results from the project made an impact, or are likely to make an impact, beyond the bounds of science, engineering, and the academic world on areas such as:

- *improving public knowledge, attitudes, skills, and abilities;*
- *changing behavior, practices, decision making, policies (including regulatory policies), or social actions; or*
- *improving social, economic, civic, or environmental conditions.*

Nothing to report.

5. **CHANGES/PROBLEMS:** The Project Director/Principal Investigator (PD/PI) is reminded that the recipient organization is required to obtain prior written approval from the awarding agency Grants Officer whenever there are significant changes in the project or its direction. If not previously reported in writing, provide the following additional information or state, "Nothing to Report," if applicable:

Changes in approach and reasons for change
Describe any changes in approach during the reporting period and reasons for these changes. Remember that significant changes in objectives and scope require prior approval of the agency.

No changes/problems to report

Actual or anticipated problems or delays and actions or plans to resolve them
Describe problems or delays encountered during the reporting period and actions or plans to resolve them.

Nothing to report.

Changes that had a significant impact on expenditures
Describe changes during the reporting period that may have had a significant impact on expenditures, for example, delays in hiring staff or favorable developments that enable meeting objectives at less cost than anticipated.

Nothing to report.

Significant changes in use or care of human subjects, vertebrate animals, biohazards, and/or select agents
Describe significant deviations, unexpected outcomes, or changes in approved protocols for the use or care of human subjects, vertebrate animals, biohazards, and/or select agents during the reporting period. If required, were these changes approved by the applicable institution committee (or equivalent) and reported to the agency? Also specify the applicable Institutional Review Board/Institutional Animal Care and Use Committee approval dates.

Significant changes in use or care of human subjects

Nothing to report.

Significant changes in use or care of vertebrate animals.

Nothing to report.

Significant changes in use of biohazards and/or select agents

Nothing to report.

there is nothing to report under a particular item, state "Nothing to Report."

6. Products:

- **Publications, conference papers, and presentations**
  Report only the major publication(s) resulting from the work under this award.

Journal publications.

1. Puca, L., et al., **Nat Commun**, 2018. 9(1): p. 2404., yes
2. Beltran, H., et al., **Clin Cancer Res**, 2018., yes
3. Beltran et al. **Clinical Cancer Research** (2019), yes
4. Puca L... Beltran H, **Science Translational Medicine** (2019), to a small degree
5. Berger, A., Brady, N … Rickman DS, **Journal of Clinical Investigation** (2019), yes
6. Beltran et al… **Clinical Cancer Research** (2019) , yes
7. Conteduca V. et al…. Beltran H**. European Journal of Cancer** (2019), yes
8. Beltran et al… **Journal of Clinical Investigation** (2020), yes
9. Brady, N., et al. …Beltran, H.,..Rickman, DS *Temporal evolution of cellular heterogeneity during the progression to advanced,* **Nat Commun**, 2018, yes

Books or other non-periodical, one-time publications.

Nothing to report.

Other publications, conference papers, and presentations. *Identify any other publications, conference papers and/or presentations not reported above. Specify the status of the publication as noted above. List presentations made during the last year (international, national, local societies, military meetings, etc.). Use an asterisk (*) if presentation produced a manuscript.*

We presented this data at the AACR – Prostate Cancer December 2017, Orlando, FL; Prostate Cancer SPORE programs Annual Retreat, February 2018, 2019, 2020 Ft. Lauderdale, FL; AACR April 2018, 2019; Society of Basic Urologic Research, Palm Beach, CA Nov 2018 and New Orleans, LA, Nov 2019.

- **Website(s) or other Internet site(s)**
  List the URL for any Internet site(s) that disseminates the results of the research activities. A short description of each site should be provided. It is not necessary to include the publications already specified above in this section.

Nothing to report.

- **Technologies or techniques**
  Identify technologies or techniques that resulted from the research activities. In addition to a description of the technologies or techniques, describe how they will be shared.

Nothing to report.

- **Inventions, patent applications, and/or licenses**
  Identify inventions, patent applications with date, and/or licenses that have resulted from the research. State whether an application is provisional or non-provisional and indicate the application number. Submission of this information as part of an interim research performance progress report is not a substitute for any other invention reporting required under the terms and conditions of an award.

Nothing to report.

- **Other Products**
  Identify any other reportable outcomes that were developed under this project. Reportable outcomes are defined as a research result that is or relates to a product, scientific advance, or research tool that makes a meaningful contribution toward the understanding, prevention, diagnosis, prognosis, treatment, and/or rehabilitation of a disease, injury or condition, or to improve the quality of life. Examples include:
  - *data or databases;*
  - *biospecimen collections;*
  - *audio or video products;*
  - *software;*
  - *models;*
  - *educational aids or curricula;*
  - *instruments or equipment;*
  - *research material (e.g., Germplasm; cell lines, DNA probes, animal models);*
  - *clinical interventions;*
  - *new business creation; and*
  - *other.*

Nothing to report.

7. PARTICIPANTS & OTHER COLLABORATING ORGANIZATIONS

What individuals have worked on the project?

Provide the following information for: (1) PDs/PIs; and (2) each person who has worked at least one person month per year on the project during the reporting period, regardless of the source of compensation (a person month equals approximately 160 hours of effort). If information is unchanged from a previous submission, provide the name only and indicate "no change."

Name: *Himisha Beltran, MD*
Project Role: *PI*
Researcher Identifier (e.g. ORCID ID):
Nearest person month worked:

Contribution to Project: *Work on Aim 1,2,3*
Funding Support:

Name: *David Rickman, PhD*
Project Role: *PI*
Researcher Identifier (e.g. ORCID ID):
Nearest person month worked: *3*

Contribution to Project: *Work on Aim 1,2,3*
Funding Support:

Name: *Brian Robinson, MD*
Project Role: *co-I*
Researcher Identifier (e.g. ORCID ID):
Nearest person month worked:

Contribution to Project: *Work on Aim 1,2*
Funding Support:

Name: *Nicholas Brady*
Project Role: *Post-doctoral fellow*
Researcher Identifier (e.g. ORCID ID):
Nearest person month worked: *3*

Contribution to Project: *Work on Aim 2*
Funding Support: *This award.*

Has there been a change in the active other support of the PD/PI(s) or senior/key personnel since the last reporting period?

1R01CA241486-01A1 (Beltran)
National Institutes of Health-National Cancer Institute, 2020-2025
Molecular mechanisms of AR Independence

1R01CA230913-01A1 (Rickman)
National Institutes of Health-National Cancer Institute, 2019-2024
Defining Molecular Determinants of Lineage Plasticity as a Mechanism of Treatment Resistance in Prostate Cancer
Roles: PI (Rickman), Co-Investigator (Beltran)
Goals/Aims: To characterize the synergy between *MYCN* induction and *RB1* loss and downstream events that promote lineage switching and treatment response at a single-cell resolution.

1R01CA179100-01A1 (Goodrich)
National Institutes of Health-National Cancer Institute, 2014-2020
NOTCH signaling controls transformation to androgen independent, neuroendocrine prostate cancer."
Role: co-Investigators (Beltran, Rickman)
Goals/Aims: To characterize the NOTCH signaling and its role in the transformation to androgen independent, neuroendocrine prostate cancer.

PC180216 (Barbieri)
Idea Development Award, US Department of Defense, Prostate Cancer Research Program, 2019-2021
Defining the Potential of Early Molecular Subtypes of Prostate Cancer to Progress to AR-Indifferent Disease
Goals/Aims: To define genomic subclasses of early PCa that are susceptible or resistant to conversion to NEPC and to determine if SPOP mutations prevent N-Myc driven conversion to NEPC using unique preclinical platforms.
Role: co-Investigators (Rickman, Beltran)

PC180637 (Giannakakou)
Idea Development Award, US Department of Defense, Prostate Cancer Research Program, 2019-2021.
Transferrin Receptor Identifies a Comprehensive Pool of Circulating Tumor Cells with Unique Molecular Features from Metastatic Prostate Cancer Patients
Goals/Aims: To examine if the transferrin receptor expression is functionally linked with N-Myc and contributes to disease progression and that TfR+-CTC provide for the first time a liquid biopsy approach that can help the diagnosis and molecular characterization of NEPC.
Role: co-Investigators (Beltran, Rickman)

P50 CA211024 Specialized Programs of Research Excellence (SPORE) (Loda)
National Cancer Institute, 08/01/2017-07/30/2022
Weill Cornell Medicine (WCM) SPORE in Prostate Cancer
Project 1: *Non-invasive clinical assay for early detection of treatment resistance in patients with metastatic prostate cancer* (Beltran/Demichelis)
Project 2: *Targeting N-MYC and EZH2-Driven Castrate Resistant Prostate Cancer* (Project Leaders: Rickman / Beltran)
Effort: 1.2 calendar (Project 1); 1.2 calendar (Project 2)
Goals/Aims Project 1: The goals of this project are to determine tumor dynamics and the clinical impact of circulating alterations in predicting response to AR-directed therapy and define the spectrum of circulating DNA alterations in patients with metastatic CRPC.
Goals/Aims Project 2: The goal of this project is to develop more effective targeting strategies for a biomarker-selected subgroup of late stage CRPC driven by N-Myc and less dependent on the AR.

W81XWH-17-PCRP-IA (Tagawa/ Beltran/ Bander)
07/01/2018-06/30/2021 0.36 calendar
Department of Defense: Prostate Cancer Research Program
Molecular and clinical correlates with prostate-specific membrane antigen (PSMA)-targeted radionuclide therapy
The goal of this project is to determine the best genomic, clinical, and imaging characteristics for successful PSMA-TRT and described immune response from PSMA-TRT. Specific Aims: 1. Prospectively and retrospectively assess genomic biomarkers and gene expression changes associated with outcome from anti-PSMA targeted radionuclide therapy. 2.

8. SPECIAL REPORTING REQUIREMENTS

COLLABORATIVE AWARDS: For collaborative awards, independent reports are required from BOTH the Initiating PI and the Collaborating/Partnering PI. A duplicative report is acceptable; however, tasks shall be clearly marked with the responsible PI and research site. A report shall be submitted to **https://ers.amedd.army.mil** for each unique award.

QUAD CHARTS: If applicable, the Quad Chart (available on https://www.usamraa.army.mil) should be updated and submitted with attachments.

9. APPENDICES:

Attach all appendices that contain information that supplements, clarifies or supports the text. Examples include original copies of journal articles, reprints of manuscripts and abstracts, a curriculum vitae, patent applications, study questionnaires, and surveys, etc.